

# Monitoring Arterial Pulse Waves With Synchronous Body Sensor Network

Mikko Peltokangas, Antti Vehkaoja, Jarmo Verho, Matti Huotari, Juha Rönning, and Jukka Lekkala

**Abstract**—A wireless body sensor network for arterial pulse wave (PW) measurements is presented and tested with ten subjects. The system is capable of recording both mechanical PW contours with sensors made of a low-cost polypropylene-based material called electromechanical film (EMFi) and volume pulse signal with photoplethysmographic transducers. By using both types of sensors, the PW contours can be recorded from various locations. The system combined with automatic analysis methods enables to easily analyze the PW contours in order to obtain a more comprehensive view on the vascular health. To demonstrate this, two parameters used in literature, reflection index and radial augmentation index were calculated for the test subjects as a function of time. The results show that these parameter values may vary more than 20% in a period of 100 s, which suggests that a large number of PWs should be analyzed before making conclusions based on the calculated indices. In addition, the effects of the static bias force to the mechanical PW signal recorded with the EMFi sensors were studied. The PW signal with the maximum amplitude is obtained when the pressure caused by the static bias force corresponds to the contact pressure between typical systolic and diastolic blood pressures. The EMFi sensors used in the proposed system are a potential low-cost alternative for tonometric sensors in collecting data in the PW analysis for arterial screening.

**Index Terms**—Body sensor networks, electromechanical sensors, photoplethysmography, pulse measurements.

## I. INTRODUCTION AND MOTIVATION

CARDIOVASCULAR diseases (CVDs) are globally the biggest cause of death, killing over 17.3 million people in 2008. The number equals to 30% of the whole mortality in that year. Unfortunately, the annual number of CVD-related deaths is still expected to rise to over 23 million by year 2030 due to aging population and unhealthy lifestyle [1]. To diagnose the latent disorders of CVDs, there is a need for an easy-to-use method to evaluate the vascular condition in order to motivate people suffering from such disorders to change their lifestyle to healthier direction or to provide them a proper medication.

Healthy elastic arteries are capable of storing energy carried by a systolic pressure pulse as a result of the left ventricular

contraction of the heart and releasing the stored energy gradually during the diastole. However, the elasticity of the arteries decreases with age, but also the unhealthy lifestyle speeds up the arterial degeneration [2]. The arteries are stiffened since the properties of the arterial wall material are changed: the elastin lamellae on the arterial wall are fatigued, becoming replaced by collagen fibers and this leads to thicker and stiffer arterial walls resulting a disease called arteriosclerosis [2]. Stiffened arterial walls are not capable of storing the energy carried by the pulse wave (PW) and this increases the systolic blood pressure (BP) and the left ventricular load [2]. The increased systolic BP stresses the stiffened arteries heavily, speeding up the degeneration of the arteries. This increases the risk of the fractures in the arterial walls that may cause severe dysfunction of vital organs, such as cerebral hemorrhage and even premature death.

Valuable information on the arterial elasticity can be obtained by analyzing arterial PW contours and pulse wave velocity (PWV) that depend on the arterial elasticity [2]–[6]. The PWV can be expressed either by using Bramwell–Hill equation [4] as

$$PWV = \sqrt{\frac{A\Delta p}{\Delta A\rho}} \quad (1)$$

or Moens–Korteweg [4] equation as

$$PWV = \sqrt{\frac{Eh}{2\rho r}}. \quad (2)$$

In (1) and (2),  $A$  and  $\Delta A$  represent the arterial lumen area and its changes due to the pulse pressure  $\Delta p$ ,  $\rho$  is the density of the blood,  $E$  and  $h$  are the Young's modulus and the thickness of the arterial wall, and  $r$  is the radius of the artery. Both equations show that the PWV is higher in degenerated stiffened arteries than in healthy elastic arteries. The dependence between the arterial elasticity and PWV provides the physical basis for the PW analysis since the observed PW is a superposition of a percussion wave that is induced by the heartbeat and its reflections from the impedance discontinuities of the central arterial network (see Fig. 1) [7]–[9]. The percussion wave and its reflections overlap in the measured PW contour (see Fig. 1), so its shape depends on the arrival times of each reflection and, thus, the PWV and the arterial elasticity.

In this study, we present a wireless body sensor network which is capable of measuring multiple channels of the PW data synchronously from different locations on the body. Also the ECG and respiration signals are simultaneously recorded by the system. The benefit of a multichannel measurement setup is that a more comprehensive view of cardiovascular health can be obtained as the PW contours differ between the different

Manuscript received November 27, 2013; revised May 26, 2014; accepted May 27, 2014. Date of publication June 4, 2014; date of current version November 3, 2014. The work was supported by the Finnish Funding Agency for Technology and Innovation (TEKES) as a part of the project Human Body Embedded Physiological Monitoring System (HealthSens, under Grant 40150/12).

M. Peltokangas, A. Vehkaoja, J. Verho, and J. Lekkala are with the Department of Automation Science and Engineering, Tampere University of Technology, 33720 Tampere, Finland (e-mail: mikko.peltokangas@tut.fi; antti.vehkaoja@tut.fi; jarmo.verho@tut.fi; jukka.lekkala@tut.fi).

M. Huotari and J. Rönning are with the Oulu University, 90570 Oulu, Finland (e-mail: matti.huotari@ee.oulu.fi; juha.ronning@oulu.fi).

Color versions of one or more of the figures in this paper are available online at <http://ieeexplore.ieee.org>.

Digital Object Identifier 10.1109/JBHI.2014.2328788

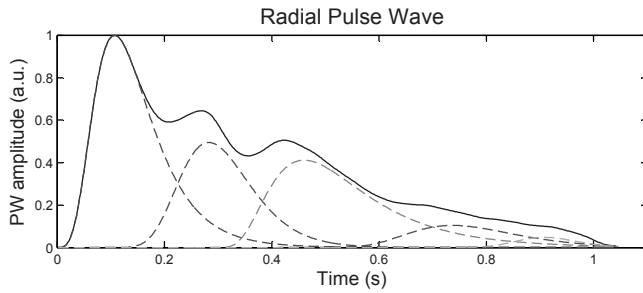


Fig. 1. Radial PW from a 24-year-old test subject. Also the principle of the overlapping of the percussion wave and its reflections is shown in dashed.

arterial sites depending on the arterial conditions and locations of possible occlusions.

## II. RELATED WORK

Current gold standard for studying the vascular condition is based on the use of ultrasonic transducers. The ultrasonic transducers are used to measure the intima media thickness of the carotid artery or detecting the pulse onsets in the carotid and femoral arteries for carotid-femoral PWV determination. However, the use of the ultrasonic device requires a skilled operator to perform the experiment, and this limits the usage of these methods in systematic vascular screening [10], [11].

In related studies, the PW refers either to a volume pulse or a pressure pulse. Thus, the data for the pulse analysis are recorded as a pressure-dependent signal with force sensors or as a peripheral blood volume dependent photoplethysmogram (PPG). The information content of these two signals is different because of a nonlinear pressure–volume dependence [12] and because of the recording sites of these two signals are usually different.

In the widely used noninvasive PPG technique, as, e.g., in [3], [6], [9], and [12], the light is focused to the tissue and the absorption of the light is determined by measuring the intensity of transmitted or scattered light. Both of them are affected by the varying peripheral blood volume caused by the pulsating blood perfusion.

Another noninvasive method for the arterial PW recordings is to place a force sensor on the pulsating artery. These kind of PW signals are traditionally recorded by using expensive high-fidelity applanation tonometry devices [2]. An alternative technique for recording pressure-related PW signals is the use of the sensors made of electromechanical film (EMFi) [9], [13]. A low unit price of the EMFi sensor enables to measure the PW signal cost effectively from multiple body locations, which is beneficial when studying the arterial condition.

In the analysis point of view, various indices derived from the PW contours have been proposed in the literature to describe the arterial condition. Takazawa *et al.* [3] proposed a parameter called aging index (AGI) which is based on the second derivative of a index finger PPG. Parameters called reflection index (RI) and stiffness index are calculated from the PPG signal based on the locations and heights of the diastolic and systolic

peaks [5]. The pressure PW contours recorded from the carotid and radial arteries have been analyzed by calculating different augmentation indices (AIx) that are based on the amplitudes of two systolic peaks [14]. However, currently the use of these parameters is mainly limited to research purposes. There are also studies that suggest different kind of PW decompositions as a startpoint for the PW analysis. In the PW decomposition, individual PW contours are presented as a sum of 2–5 highly nonlinear basis functions [6], [9], [15], [16].

Without automatic analysis methods, the results of PW contour analysis are often studied only for a relatively short period of PW signal by using a small number of PW contours. However, the beat-to-beat variation of the indices can be high even for healthy subjects. For instance, the difference between the AGI values computed from two consecutive PW contours can be as high as 39% of the whole scale of the AGI [17].

## III. MEASUREMENT SETUP

Our PW measurement system consists of wireless sensor nodes and a network coordinator that communicates with a computer through the USB. The synchronous sensor network is partially based on the IEEE 802.15.4 standard and it uses time division multiple access as the mechanism for the bandwidth management. The maximum number of sensor nodes in one measurement network is 8 and the transfer distance is approximately 50 m with full transmit power (0 dBm) in open field.

In the proposed system, there are three different types of sensor nodes: 1) two-channel force sensor nodes for pressure PW measurements (see Fig. 2), 2) one-channel PPG nodes for volume pulse measurements as well as, and 3) ECG and respiration nodes. Each force sensor channel is equipped with a dynamic force sensor and a piezoresistive static force sensor (see Fig. 2). The dynamic force sensors are used for the PW measurements, whereas the static force sensors can be utilized in adjusting the proper static bias force that flattens the artery for obtaining good-quality PW signal.

The sample rate for the dynamic force sensors is 250 Hz and for the static force sensors 10.4 Hz. The PPG sensor nodes measure one channel with 500-Hz sample rate and the ECG/respiration nodes one ECG lead and one respiration channel with 250 Hz each. The recorded signals are sampled synchronously by using a 16-bit analog-to-digital converter. The network structure includes additional transmission time slots for retransmissions, thus allowing an average packet loss rate of up to 25% without losing the data. When analyzing the recorded signals, it was found that only 0.02% of the total amount of data was lost in the wireless data transmission.

### A. Force Sensor Nodes

The dynamic force sensors for the PW measurements are made of a material called EMFi. EMFi is a permanently charged electret material and consists of multiple polypropylene layers separated by air voids [18]. When an external dynamic force is applied on a piece of EMFi, the thickness of the air voids changes, modifying the internal charge distribution that causes

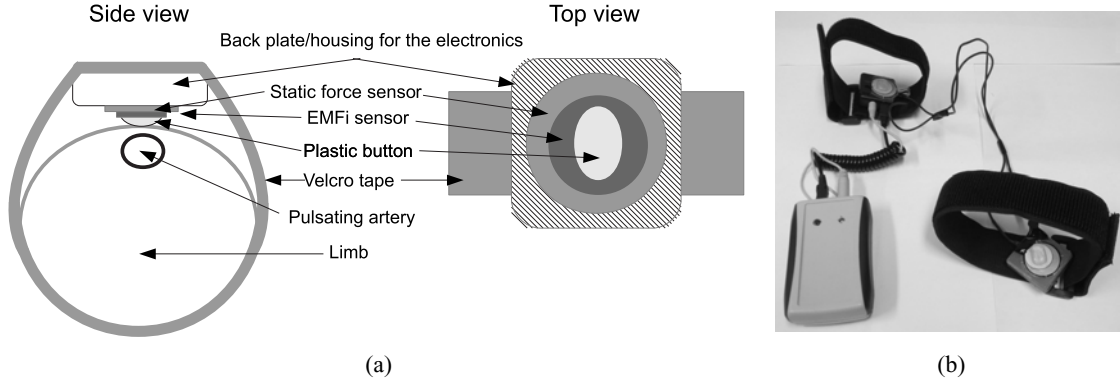


Fig. 2. a) Side and top views for the force sensor node and its placement on the artery. The EMFi sensor is under the plastic contact piece and the piezoresistive static force sensor is under the EMFi sensor. b) Photograph of a force sensor node with two sensors.

a displacement charge to the electrodes covering the surfaces of EMFi. The charge  $\Delta q$  generated by a dynamic force  $\Delta F$  exerted on EMFi sensor is expressed as

$$\Delta q = S \Delta F \quad (3)$$

where  $S$  is the sensitivity. The charge is turned into voltage  $\Delta V$  as

$$\Delta V = \frac{S \Delta F}{C} \quad (4)$$

where  $C$  is the capacitance seen at input of a voltage amplifier. [18]

The schematic and photographic presentations of a force sensor node are shown in Fig. 2. The circular EMFi sensors used in our system have a diameter of 20 mm. However, having a direct skin contact with this large sensor does not produce good-quality PW signals. For this reason, a rounded plastic contact piece having the contact area of approximately half of the sensor area is attached on each sensor to press the pulsating artery and to focus the force transmission from the artery to the sensor. Each EMFi sensor is fixed on a rigid backplate with a piezoresistive static force sensor (FlexiForce A401 by Tekscan). The sensors with the rigid backplate are fixed on each measurement point by using textile bands around the limbs.

To verify that the mass of the contact piece does not affect the spectral content of the recorded mechanical PW signal, additional measurements with another type of EMFi sensor with a direct skin contact were performed. As a result of these experiments, the spectral contents and scaled time domain presentations of the simultaneously measured signals were found to be equivalent.

In the electronics point of view, the preamplifier stage of the EMFi sensors is a noninverting voltage amplifier, and the total voltage gain of the EMFi signal is 13.2. This corresponds roughly to the sensitivity of 1 V/N in our measurement setup. The passband of the EMFi signals is limited to 50 mHz–100 Hz.

### B. Force Sensor Placement

Eight EMFi sensors (Emfit Ltd.) are used on different arterial locations as shown in Fig. 3. The measurement sites for the EMFi sensors are both wrists (radial arteries) and the bends

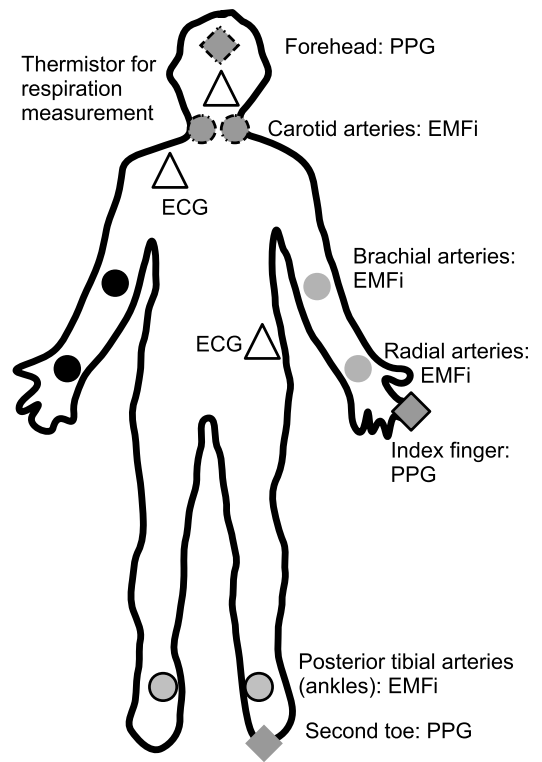


Fig. 3. Sensor placement. The measurement sites with the similar marker indicate that the sensors placed on these points are connected to the same sensor node.

of the arms (brachial arteries), the neck (left and right common carotid arteries), and both ankles (posterior tibial arteries). These measurement sites were selected due to the existence of a large artery near the skin surface.

### C. PPG, ECG, and Respiration Measurements

While four sensor nodes of eight are equipped with the force sensors, three nodes are used for the PPG measurements and one node for the ECG and respiration measurements. Each PPG node measures the transmitted or scattered infrared (IR) light (wavelength 905 nm) with a photodiode. Two of the PPG sensors

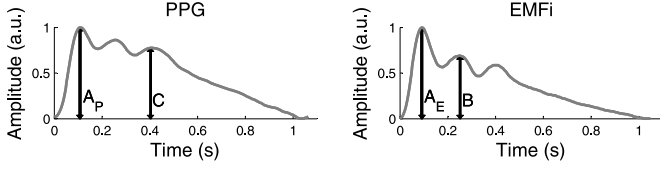


Fig. 4. Early systolic peak  $A_P$  and diastolic peak  $C$  for the PW obtained from PPG signal from left index finger (left panel) and early systolic peak  $A_E$  and late systolic peak  $B$  for the PW recorded with EMFi sensor the left wrist (right panel).

are used to record transmitted IR light through the index finger and the second toe (see Fig. 3). The third PPG sensor measures the scattered IR light on the forehead (see Fig. 3). The low-frequency baseline variations of the PPG signals are high-pass filtered with a cutoff frequency of 0.15 Hz.

Bipolar ECG is recorded by two disposable Ag/AgCl electrodes placed under the right clavicle and on the left lower abdomen (see Fig. 3). The ECG is used in recording the heart rate and to assist in the PW detection for further analysis. The ECG signal is recorded by using a passband of 0.2–40 Hz.

Because the respiration normally affects the heart rate and also the PWV, the other channel of the ECG node is equipped with an NTC thermistor integrated into a respiration mask. The recorded respiration signal is bandpass filtered for a band of 3.4 mHz–40 Hz.

#### IV. TEST MEASUREMENTS AND DATA PROCESSING

The system was tested on ten subjects. The ages of the subjects were 22–64 years and they were healthy without diagnosed cardiovascular disorders. The measurements were made in supine posture and the data were collected for at least 10 min. The goal of these measurements was to determine which measurement points provide the best signal for the PW analysis, as well as to see how much there are variations over the time in the parameters extracted from the PW signals. In addition, we validated the suitability of the EMFi sensors for the PW recording. In that experiment, we compared the pulse signal recorded with EMFi to the pulse signal simultaneously recorded with a commercial SphygmoCor applanation tonometer from test subject 6.

The values of two parameters, RI, and radial augmentation index (rAIx), were calculated for all subjects for a 100-s period in order to see how the features of PW contours vary with time. The RI is calculated as the ratio of the amplitudes of the diastolic ( $C$ ) and the systolic ( $A_P$ ) waves of the PPG signal from the left index finger (see Fig. 4) as [5]

$$RI = \frac{C}{A_P} \quad (5)$$

and the rAIx is calculated as the ratio of the amplitudes of early ( $A_E$ ) and late ( $B$ ) systolic waves of the EMFi signal from the left wrist as [14]

$$rAIx = \frac{B}{A_E} \quad (6)$$

The amplitudes  $A_P$ ,  $A_E$ ,  $B$ , and  $C$  are illustrated in Fig. 4. If the PW contour does not have a local maximum at point  $B$  or  $C$ ,

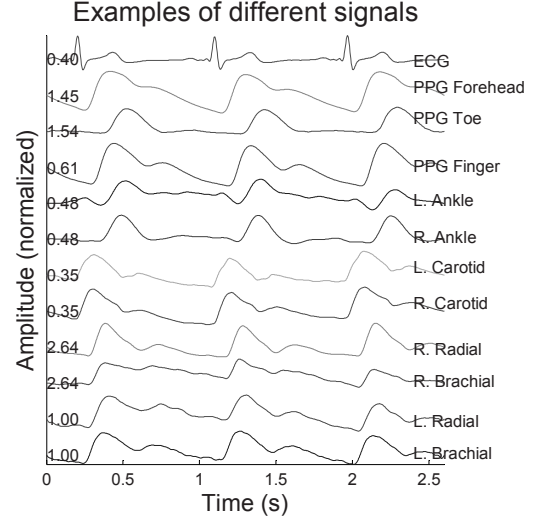


Fig. 5. Examples of PW signals from different measurement points from a 25-year-old man. The signals are normalized by dividing with the normalization factors shown on the left.

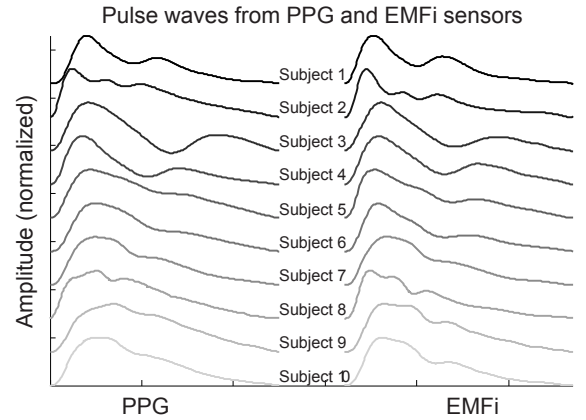


Fig. 6. Examples of normalized PW contours for each test subject from the index finger PPG signal and from the radial artery EMFi signal.

higher order derivative analysis is performed to find the values of  $B$  and  $C$  [14].

Further, the effects of the static bias force on the EMFi sensor signal from the radial artery were studied. These measurements were performed by placing the EMFi sensor on the radial artery as normally, and then inserting a set of plastic plates between the wristband and the dorsal site of the arm. The plastic plates were removed one-by-one in order to gradually decrease the static bias force.

#### V. RESULTS AND DISCUSSION

##### A. Signals From Different Measurement Points

Examples of recorded good-quality PW signals from different locations are shown in Fig. 5. In addition, PW signals from the left index finger (PPG) and the radial artery (EMFi) are shown in Fig. 6 for each test subject. The shape of the



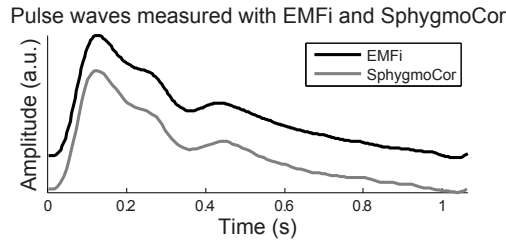


Fig. 7. Examples of PW contours recorded from subject 6 with EMFi (right wrist) and Sphygmocor tonometer (left wrist) show very similar characteristics.

recorded PW contours varies between different measurement sites (see Fig. 5), between different body positions, from person to person (see Fig. 6) and between different sensor modalities. The signal amplitudes are normalized in Figs. 5 and 6, but the actual amplitudes of the signals from different recording sites may vary about one order of magnitude. In all test subjects, the mechanical PW signals with the best signal-to-noise ratios were recorded from the wrists and the bends of the arms. Also all the PPG signals from the forehead, index finger, and the second toe were clear for visual interpretation. For some test subjects, finding the correct placement for the EMFi sensor at ankles and neck was challenging. Thus, the PW signals from the upper limbs seem to be more suitable, e.g., for the quick screening of the cardiovascular system.

Even though it is possible to record PWs from various measurement points, the analysis methods found in the literature have been proposed mainly for the radial PWs and finger PPGs. However, the measurement and analysis of the PW signals also from the lower limbs could be a useful tool in studying the risk for the vascular diseases (e.g., intermittent claudication) or the severity of the diseases that cause symptoms only in the lower limbs [19].

### B. Comparison Between EMFi and Applanation Tonometer

The differences between the PW contours recorded with EMFi sensors and a commercial applanation tonometry device were studied. Based on our test, the very similar features are widely seen in both sensor signals as in the example shown in Fig. 7. This suggests that the EMFi is a potential low-cost alternative for recording data for the PW analysis for the vascular health evaluation. However, the EMFi sensors are only sensitive to dynamic forces whereas the tonometric sensors measure also static forces. This limits the suitability of EMFi sensors, e.g., for tonometric BP measurements.

### C. Reflection Index (RI) and Radial Augmentation Index (rAIx)

Beat-to-beat variability of the selected parameters, RI and radial AIx (rAIx), were studied by computing their values for each heart beat for a 100-s period. The RI is calculated from the index finger PPG signal, whereas the rAIx is obtained from the EMFi signal from the left wrist. The results for the RI and rAIx are shown along with the respiration sensor output in Fig. 8.

Although some of the most spiky features in Fig. 8 are caused by errors in the automated signal processing, the notable beat-to-

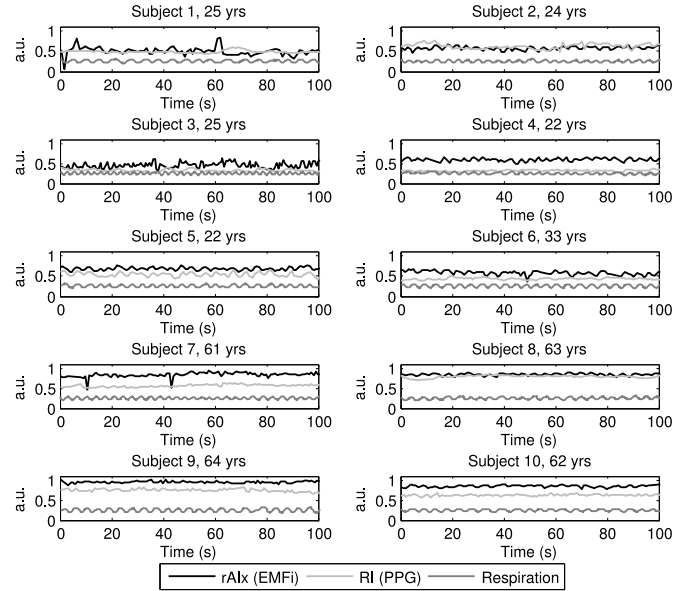


Fig. 8. RI and rAIx as a function of time for each test subject. Also the output of the respiration sensor is shown.

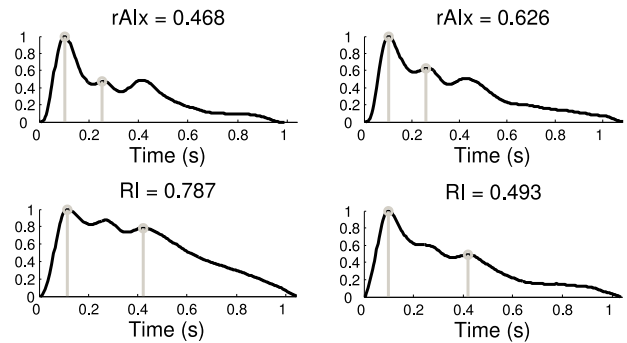


Fig. 9. Examples of the rAIx and RI determination from the different PWs of test subject 2 show that the parameter values vary from PW to PW.

beat variation (see Fig. 9) of both parameters indicates that the analysis of a large number of PW contours could provide a more reliable view on the vascular health than the analysis of only a small number of individual PW contours. For instance, test subject 1 has a temporary rise of approximately 20% in the value of RI at 60–75 s. In addition to this, there are clear respiration-synchronous variations in the parameter values with most of the subjects. Therefore, the analysis of only individual PW contours may lead to totally wrong conclusions of the subject's vascular health.

For 22-year-old test subjects 4 and 5, the values of rAIx time series are much closer to each other than the values of their RI time series. This could be explained by the fact that pressure and volume PWs are not linearly dependent on each other [12]. Furthermore, the variation in the characteristics of the PW morphology is wide from person to person as shown in Fig. 6. For this reason, we believe that not only the arterial condition but also other physiological reasons, such as BP or the exact anatomical structure of arterial tree, may also affect

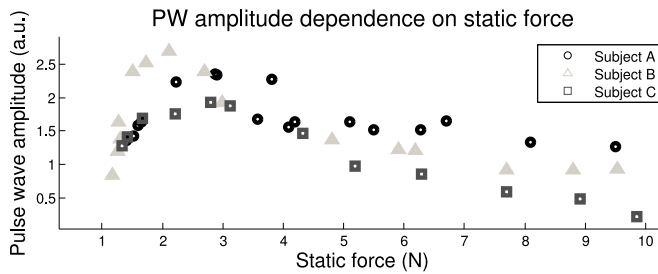


Fig. 10. Dependence of the mean radial artery PW amplitude on the supporting bias force for three test subjects.

to the PW morphology. Thus, single simple features such as RI or rAIx should not be used alone to evaluate the arterial condition. In this point of view, the automatic analysis methods that produce multiple parameters from the PW signals measured from the various arterial sites with different techniques could provide better understanding on the vascular condition. Also novel parameters based on, e.g., the PW decomposition analysis could provide additional information on the vascular health.

#### D. Effects of Static Force

It was observed in the test measurements that the strength of the effects of the static bias force to the PW amplitude are personal and probably depend on the structure of the measurement site. The effects of the static bias force may be affected also by the skin-sensor contact and the temporary variations in the BP levels. In an earlier study,  $\pm 40\%$  change in the static force caused as high as 80% decrease in PW amplitude [20]. The amplitude of the PW contour recorded with a PPG probe on the left index finger was not affected by the bias force of the EMFi sensor on the left wrist that shows that the two sensor modalities can be safely colocated to the same limb.

When the static bias force is too small, the sensor does not stay on the measurement site or does not flatten the artery enough. In an opposite case, the EMFi sensor with too high bias force occludes the artery and attenuates its pulsations. The most optimal static bias force is typically 2–3 N (see Fig. 10). These forces correspond to the contact pressures of 90–140 mmHg for the sensing area of approximately  $1.6 \text{ cm}^2$ , and these contact pressures are between the typical systolic and diastolic BP readings. In such situation, the total loading of the arterial wall reaches its minimum.

Besides the PW amplitude, also the shape of the PW contour is affected by the bias force as seen in Fig. 11. If the applied bias force is too high, the PW morphology is distorted: in Fig. 11, the level of the dicrotic notch falls even under the baseline of the PW signal. The changes in the PW contour morphology are even more important aspects than the changing amplitude when calculating the indices based on the waveform of individual PWs.

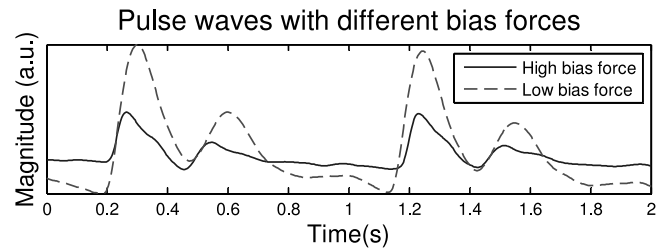


Fig. 11. Radial PW contours with optimal and too high bias forces from the same test subject.

## VI. CONCLUSION

A wireless synchronous body sensor network for the arterial PW measurements is presented. The system allows to record both mechanical PW signals by using EMFi sensors and volume pulse signals by using PPG transducers. Both types of signals provide valuable information about the arterial elasticity. Because the signals recorded with the EMFi sensors follow the shape of PWs recorded with a commercial pressure transducer, the EMFi is a potential low-cost alternative for expensive tonometric sensors. However, when using the EMFi sensor, it is important to adjust the static bias force that flattens the artery to an appropriate level to obtain the PW signal without distortion.

Especially, the mechanical PW signals recorded from the upper limbs have a high signal-to-noise ratio. The signals recorded from the lower limbs are more challenging to record although they could provide additional information on the vascular diseases related to the lower limbs. When studying the indices derived from the individual PW contours, the values of the parameters contain notable variations even in as short as a 100-s period, caused not only by the respiration but also by the fluctuations of the autonomous nervous system. For this reason, advanced automatic analysis methods could provide a more comprehensive view on the cardiovascular health than a manual analysis of a small number of PW contours. However, more studies are needed to verify the clinical significance of the data recorded with the proposed system.

## ACKNOWLEDGMENT

The authors would like to thank all the volunteer test subjects for their valuable contribution to the study.

## REFERENCES

- [1] A. Alwan, and World Health Organization, *Global Status Report on Non-communicable Diseases 2010*. Geneva, Switzerland: World Health Organization, 2011.
- [2] M. F. O'Rourke and J. Hashimoto, "Mechanical factors in arterial aging: A clinical perspective," *J. Amer. College Cardiol.*, vol. 50, no. 1, pp. 1–13, 2007.
- [3] K. Takazawa, N. Tanaka, M. Fujita, O. Matsuoka, T. Saiki, M. Aikawa, S. Tamura, and C. Ibukiyama, "Assessment of vasoactive agents and vascular aging by the second derivative of photoplethysmogram waveform," *Hypertension*, vol. 32, no. 2, pp. 365–370, 1998.
- [4] N. Westerhof, N. Stergiopoulos, and M. Noble, *Snapshots of Hemodynamics: An Aid for Clinical Research and Graduate Education*. New York, NY, USA: Springer, 2010.

- [5] S. C. Millasseau, J. M. Ritter, K. Takazawa, and P. J. Chowienzyk, "Contour analysis of the photoplethysmographic pulse measured at the finger," *J. Hypertension*, vol. 24, no. 8, pp. 1449–1456, 2006.
- [6] U. Rubins, "Finger and ear photoplethysmogram waveform analysis by fitting with Gaussians," *Med. Biological Eng. Comput.*, vol. 46, no. 12, pp. 1271–1276, 2008.
- [7] M. C. Baruch, D. E. Warburton, S. S. Bredin, A. Cote, D. W. Gerdt, and C. M. Adkins, "Pulse decomposition analysis of the digital arterial pulse during hemorrhage simulation," *Nonlinear Biomed. Phys.*, vol. 5, no. 1, pp. 1–15, 2011.
- [8] R. D. Latham, N. Westerhof, P. Sipkema, B. J. Rubal, P. Reuderink, and J. P. Murgo, "Regional wave travel and reflections along the human aorta: A study with six simultaneous micromanometric pressures," *Circulation*, vol. 72, no. 6, pp. 1257–1269, 1985.
- [9] M. Huotari, A. Vehkaoja, K. Määttä, and J. Kostamovaara, "Photoplethysmography and its detailed pulse waveform analysis for arterial stiffness," *J. Struct. Mech.*, vol. 44, no. 4, pp. 345–362, 2011.
- [10] M. L. Bots, A. W. Hoes, P. J. Koudstaal, A. Hofman, and D. E. Grobbee, "Common carotid intima-media thickness and risk of stroke and myocardial infarction: The rotterdam study," *Circulation*, vol. 96, no. 5, pp. 1432–1437, 1997.
- [11] J. Sugawara, K. Hayashi, T. Yokoi, and H. Tanaka, "Carotid-femoral pulse wave velocity: Impact of different arterial path length measurements," *Artery Res.*, vol. 4, no. 1, pp. 27–31, 2010.
- [12] J. Talts, R. Raamat, and K. Jagomägi, "Asymmetric time-dependent model for the dynamic finger arterial pressure-volume relationship," *Med. Biological Eng. Comput.*, vol. 44, no. 9, pp. 829–834, 2006.
- [13] J. Alametsä, A. Palomäki, and J. Viik, "Short and longer term repeatability of ballistocardiography in a sitting position with EMFI sensor," *Med. Biological Eng. Comput.*, vol. 49, no. 8, pp. 881–889, 2011.
- [14] V. Melenovsky, B. A. Borlaug, B. Fetis, K. Kessler, L. Shively, and D. A. Kass, "Estimation of central pressure augmentation using automated radial artery tonometry," *J. Hypertension*, vol. 25, no. 7, pp. 1403–1409, 2007.
- [15] D. Goswami, K. Chaudhuri, and J. Mukherjee, "A new two-pulse synthesis model for digital volume pulse signal analysis," *Cardiovascular Eng.*, vol. 10, no. 3, pp. 109–117, 2010.
- [16] L. Wang, L. Xu, S. Feng, M. Q.-H. Meng, and K. Wang, "Multi-gaussian fitting for pulse waveform using weighted least squares and multi-criteria decision making method," *Comput. Biology Med.*, vol. 43, no. 11, pp. 1661–1672, 2013.
- [17] K. Pilt, R. Ferenets, K. Meigas, L.-G. Lindberg, K. Temitski, and M. Viigimaa, "New photoplethysmographic signal analysis algorithm for arterial stiffness estimation," *Scientific World J.*, vol. 2013, p. 9, 2013.
- [18] J. Lekkala, and M. Paajanen, "Emfi-new electret material for sensors and actuators," in *Proc. 10th Int. Symp. Electrets*, 1999, pp. 743–746.
- [19] S. A. Carter, "Indirect systolic pressures and pulse waves in arterial occlusive disease of the lower extremities," *Circulation*, vol. 37, no. 4, pp. 624–637, 1968.
- [20] M. Peltokangas, J. Verho, T. Salpavaara, and A. Vehkaoja, "Non-invasive system for mechanical arterial pulse wave measurements," in *Proc. XIII Mediterr. Conf. Med. Biol. Eng. Comp.*, 2014, pp. 1493–1496.

Authors' photograph and biography not available at the time of publication.